Prediction of nitrogen and phosphorus contents in citrus leaves based on hyperspectral imaging

Liu Yanli[1,2], Lyu Qiang[2], He Shaolan[2], Yi Shilai[2], Liu Xuefeng[2], Xie Rangjin[2], Zheng Yongqiang[2], Deng Lie[2*]

(1. *College of Horticulture and Landscape, Southwest University, Beibei, Chongqing 400715, China*;
2. *Citrus Research Institute, Southwest University-Chinese Academy of Agricultural Sciences, Beibei, Chongqing 400712, China*)

Abstract: The nutritional status of citrus leaves is very important to the determining of fertilization plans. The spectrum technique is a quick, un-injured method and is becoming widely used for plant nutrient estimation. The possibility and method of using spectrum technique to estimate the nutrient of citrus leaf was explored in this study. A total amount of 135 leaves from the mature spring shoots of navel orange trees (*C. sinensis* Osbeck, "Newhall") were collected and randomly grouped into two sets of samples: 100 leaves for the calibration set and 35 leaves for the prediction set. The hyperspectral images were scanned upper and lower side of each leaf and then the total nitrogen (N) and phosphorus (P) contents of each leaf were measured. The raw spectra data were extracted to generate average spectra curves, preprocessed with five different methods, and was used to build N and P content prediction models. The performances of the five preprocessing methods, i.e., Savitzky-Golay smoothing (SGS), standard normal variate (SNV), multiplicative scatter correction (MSC), first-derivative (1-Der) and second-derivative (2-Der), were tested with linear partial least squares (PLS) models and nonlinear least squares-support vector machine (LS-SVM) models. The results showed that the SG-PLS and PLS were the best for the N predicting (Rp=0.9049, *RMSEP*=0.1041) and P (Rp=0.9235, *RMSEP*=0.0514) in citrus leaves, respectively; the hyperspectral image data from leaf's upper side predicting better for the contents of N and P. The study suggested that the hyperspectral image data from the upper side of the citrus leaves are suitable for nondestructive estimation of nutrient content.

Keywords: citrus leaves, nitrogen, phosphorus, prediction, hyperspectral imaging
DOI: 10.3965/j.ijabe.20150802.1464

Citation: Liu Y L, Lyu Q, He S L, Yi S L, Liu X F, Xie R J, et al. Prediction of nitrogen and phosphorus contents in citrus leaves based on hyperspectral imaging. Int J Agric & Biol Eng, 2015; 8(2): 80－88.

1 Introduction

As the most important nutrient elements, excess or insufficiency of N and P in leaves will both affect the growth and development of the plants. Hence, a real-time and accurate estimation for their nutrition levels is essential to fertilize to help achieving higher yield, better quality, and minimize water pollution from excessive fertilizers usage[1].

Received date: 2014-09-29 **Accepted date:** 2015-02-21

Biographies: Liu Yanli, Master, Research interest: fruit information technology, Email: liuyanli.1234@163.com. **Lyu Qiang**, PhD, Associate Professor, Research interest: agricultural mechanization, Email: lvqiang@cric.cn. **He Shaolan**, Associate Professor, Research interest: fruit tree physiology, Email: heshaolan@cric.cn. **Yi Shilai**, Master, Associate Professor, Research interest: fruit information technology, Email: yishilai@cric.cn. **Liu Xuefeng**, Master, Research interest: fruit information technology, Email: 1152753665@qq.com. **Xie Rangjin**, PhD, Associate Professor, Research interest: fruit tree physiology, Email: xierangjin@cric.cn. **Zheng Yongqiang**, PhD, Associate Professor, Research interest, fruit tree physiology, Email: zhengyongqiang@cric.cn.

∗**Corresponding author: Deng Lie**, Professor, Research interest: fruit physiology and information technology, Citrus Research Institute, Southwest University-Chinese Academy of Agricultural Sciences, Beibei, Chongqing 400712, China; Tel.: +86-23-68349706; Fax: +86-23-68349712. Email: liedeng@163.com.

Generally, the measuring method of N and P content in leaves is chemical analysis, which is costly, time consuming and laborious, as well as the leaves will be destructed and unsuitable for the continuously monitoring in the field. Therefore, a rapid and nondestructive method of N and P content measurements is practically needed.

Hyperspectral imaging technique has been widely applied in quantitative and qualitative analysis in agriculture, food, medicine and other industrial fields as a nondestructive, low cost and reliable detection method[2-4]. Some studies utilized visible and near-infrared spectral reflectance from plant leaves or canopies to detect moisture content and nutrient stress. Furthermore, Min et al.[5] focused on developing sensors to predict nutrition concentrations from single orange leaf. Based on the previous studies[6-8], they selected chlorophyll and protein spectral absorption bands (620-950 nm and 1 400-2 500 nm) for the sensor and designed a reflectance housing to block environmental noise and ensure single leaf measurement. The nitrogen sensor could classify unknown leaf samples into low, medium and high nitrogen levels with 70% accuracy. Considering the differences in color, exposure to light during growth, stomata distribution, other structural and biochemical traits, the upper and the lower sides of the leaves must be different in spectroscopy as shown by their respective near-infrared spectra[9-10]. The results of multiple regression analysis (MRS) of the spectra from both sides of tomato leaves showed that the spectra in the lower side of leaves were better in predicting chlorophyll content of leaves[11]. Similarly, better significant positive correlations of chlorophyll content with B, B/R, b, b/r values of the RGB system, and with the saturation(S) values of the HIS color system were observed on the lower side than on the upper side of the leaves[12]. The results indicated that using images of the lower side of a rice leaf was easier to measure the leaf area than using the traditional computer vision technology[13]. There are quite a few researches had been done on the technique for measuring the nutritional status of leaves, but few research results had been reported to compare the prediction accuracy of hyperspectral images collected from the lower and upper side of a leaf.

The objectives of this study were as follows: 1) explore the possibility of using hyperspectral imaging technique (400-1 000 nm) to determine the nutritional contents (nitrogen and phosphorus) in citrus leaves; 2) evaluate the performance of different spectral data preprocessing methods, including Savitzky-Golay (SG) smoothing, standard normal variate (SNV), multiplicative scatter correction (MSC), first-derivative (1st-Der), and second-derivative (2nd-Der); 3) determine which side of a leaf (upper vs lower) is better to predict nitrogen and phosphorus content, and 4) compare the prediction accuracy of linear partial least squares (PLS) model with t nonlinear least squares-support vector machine (LS-SVM) model.

2 Materials and methods

2.1 Sample preparation

Newhall navel orange (*Citrus sinensis* Osbeck*),* a leading navel orange cultivar in China, was used in this experiment. The trees were grown in the experimental field of the Citrus Research Institute, Chinese Academy of Agricultural Sciences, Chongqing, China (29.81°N, 106.40°E). Leaves were collected from spring shoots that reached full maturity in mid-September, 2013. Leaves were kept in ice-box and taken immediately back to the lab. A total of 135 leaves were used and their hyperspectral data were collected within 6 h.

2.2 Hyperspectral image collection

2.2.1 Hyperspectral imaging system

Hyperspectral data were obtained by using the hyperspectral imaging system (Figure 1). The system was mounted with following components: 1) a spectrograph (ImSpector V10E, Finland), 2) an electron-multiplying charge-coupled device (EMCCD) camera (Raptor photonics, FA285-CL, England), 3) a lighting system with two halogen lamps (150 W/21 V, Illumination Technologies, Inc, USA), 4) an electric controlled mobile platform, and 5) a main-control computer. The first 4 components were enclosed in a whole enclosure.

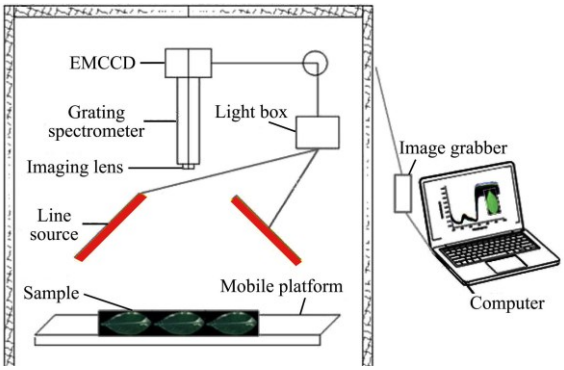

Figure 1 Hyperspectral imaging system used in this study

2.2.2 Image acquisition and correction

Hyperspectral images were collected by the system in a wavelength range of 400-1 000 nm with a spectral resolution of 2.8 nm. Leaves were fixed on a black cardboard with negligible reflectance and then placed on the mobile platform. During image acquisition, the mobile platform for line scanning had an optimized velocity of 1.78 mm/s, and the camera exposure time was 60 ms. A corrected hyperspectral image was calculated using the following equation:

$$R_c = \frac{R_s - R_d}{R_w - R_d} \quad (1)$$

where, R_c was the relative reflectance image; R_s was the sample image; R_w was the white image and R_d was the dark image. R_w was obtained using a standard white board with 99% reflectance, and R_d was acquired by covering the lens with a cap.

2.2.3 Software

Image acquisition was controlled by imaging data acquisition software (Spectral Image software, Isuzu Optics Corp., Taiwan, China) and image correction was done using software HSI Analyzer (Isuzu Optics Corp., Taiwan, China). Spectral data were extracted with ENVI 4.7 (The Environment for Visualizing Images, ITT Visual Information Solutions Corp., USA), and analyzed using the Unscrambler software (version 9.7, CAMO, ASA, Norway) and Matlab R2010a (The Mathworks, Inc., Natick, MA, USA).

2.3 Measurement of leaf nitrogen and phosphorus content

Following hyperspectral image collection, leaves were placed immediately into an oven at 105°C for 20 min to inactivate enzymes, and then let cooled to 75°C to dry until constant weight. The dry leaves were individually ground into fine powder. The powder of each leaf was weighed and wet digested in 5 mL of concentrated sulfuric acid at room temperature overnight. Sulfuric acid/hydrogen peroxide digestion and colorimetric determination was used to determine total content of phosphorus and nitrogen in each leaf[14-15]. Concentrations of nitrogen and phosphorus were calculated. The quantity unit for nitrogen and phosphorus contents shown in tables and figures is the percentage of dry weight (%).

2.4 Modeling

2.4.1 Spectral data extraction

As shown in Figure 2, A_1 and B_1 were the RGB (R: 650 nm, G: 550 nm, B: 450 nm) images of the upper and the lower side of the same citrus leaf, respectively. Apparently, the upper side (A_1) had stronger reflection areas than the lower side (B_1). A rectangular region of interest (ROI) was manually selected for both sides of leaf. Double thresholds segmentation method was employed to obtain the grey images of A_2 and B_2 by adding the corresponding blue band (480 nm) and red band (760 nm). ROIs (within A_3 and B_3) were extracted from areas with gray levels between 0.45 and 0.70. The average reflectance spectrum was calculated from the ROIs of both images by averaging the spectral values of all pixels.

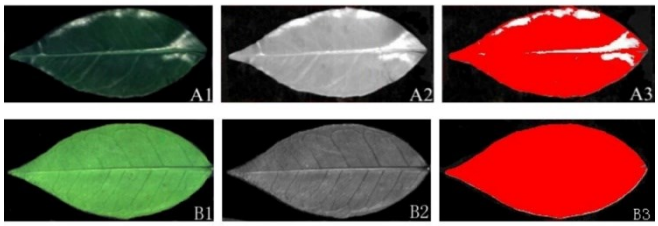

A_1, B_1: RGB images (R: 650 nm, G: 550 nm, B: 450 nm) of the upper side and the lower side of the same leaf; A_2, B_2: Sum image of 480 nm and 760 nm images; A_3, B_3: Effective region segmentation of leaf.

Figure 2 Effective region segmentation of leaf samples

2.4.2 Spectral features of citrus leaves

The spectrums reflect curves for both the upper and the lower leaf sides were extracted from ROI images (Figure 3). The highest difference in reflectance between the upper and the lower sides was at 550 nm of green wavelength where the lower side was significantly higher than the upper side. This may be related to a

lower level of pigmentation in the lower side. In the near-infrared wavelengths of 760-1 000 nm, where a high reflective platform was formed, the reflectance of lower side was slightly lower than which of the upper side, indicating that the leaf spectra could be related to internal concentrations of biochemical's and to structures of leaves[16].

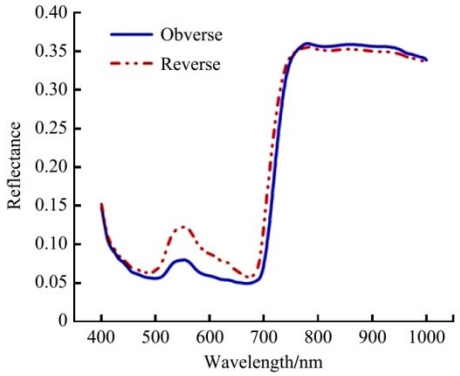

Figure 3 The reflective spectra of upper side and lower side of a same leaf

2.4.3 Results of Spectral preprocessing

Spectral pretreatment is usually performed to mathematically treat the extracted spectral data correct undesired effects such as light scattering and random noise resulting from variable physical sample properties or instrumental effects[17]. Results from various preprocessing methods, including SG smoothing, SNV, MSC, 1st-Der and 2nd-Der, were compared in the calibration stage. SG, SNV and MSC were used for de-noising, light scatter correction and light path length correction[18]. Derivatives were applied to correct the baseline shift[19]. All the preprocessing methods were implemented with "The Unscrambler V 9.8" (CAMO AS, Oslo, Norway).

2.4.4 Calibration models

Both the linear and the nonlinear calibration methods were used to retrieve the relationships between spectral data (X-variables) and nitrogen and phosphorus content (Y-variables). PLS analysis was used for linear calibrations[20] and LS-SVM was used for nonlinear calibrations[21].

For PLS modeling, the input X-variables (spectral data) were extracted into new eigenvectors (latent variables, LVs) to represent the most relevant information in the original spectra. A full cross-prediction process was used to construct a stable and robust PLS model. The prediction performance was evaluated by the samples in the prediction set.

The free LS-SVM toolbox (LSSVM V1.5, Suykens, Leuven, Belgium) was applied to develop LS-SVM models and the details of this method could be found in previous studies[22-24]. The method employed a set of linear equations using support vectors instead of quadratic programming problems to reduce the complexity of optimization processes. The input variables were settled by preprocessing methods, and radials basis function (RBF) kernel was used as the kernel function because it can reduce the computational complexity in handling nonlinear correlations and give a good performance under general smoothness assumptions. The model parameters of gamma (γ) and sigma^2 (σ^2) were settled by a two-step grid search technique with the use of leave-one-out cross-prediction. The LS-SVM algorithm was implemented by Matlab.

The prediction performance was mainly evaluated by following indices: correlation coefficients of calibration (Rc) and prediction (Rp), root mean squares error (*RMSE*) of calibration (*RMSEC*) and prediction (*RMSEP*). The *RMSE* was calculated as:

$$RMSE = \sqrt{\frac{\sum_{i=1}^{n}(\hat{y}_i - y_i)^2}{n}} \quad (2)$$

where, n was the number of samples; and y_i and $\hat{y}_i$ were the reference and predicted values of the i^{th} leaf, respectively.

3 Results and discussion

3.1 Nutritional analysis

All of 135 leaves collected for hyperspectral images were individually analyzed for their N and P levels. one hundred of leaves were randomly selected as calibration set, and the remaining 35 leaves were used as the prediction set. No leaf was used in both calibration set and prediction set. As shown in Table 1, the distribution of nitrogen and phosphorus content in the calibration sample set is consistent with that in the prediction sample set, and the difference between the two sets is very small. This indicates that our data is available for the building of predicting models for N and P content in leaves.

Table 1 Total nitrogen and phosphorus content in the calibration and prediction sample sets

Nutrient element	Sample set	Leaves	Mean /%	Min /%	Max /%	Standard deviation
Nitrogen	Calibration	100	2.53	2.37	3.11	0.2587
	Prediction	35	2.59	2.46	3.06	0.2753
Phosphorus	Calibration	100	0.15	0.11	0.17	0.0158
	Prediction	35	0.14	0.12	0.17	0.0155

3.2 PLS models

Different PLS models were built using the aforementioned preprocessing methods and evaluated by *R*p and *RMSEP*. As shown in Table 2, compared with other preprocessing methods, SG got the highest *R*p and the lowest *RMSEP* and can be considered as the best preprocessing method. The spectral data from the upper side of the leaf is better than the lower side. The optimal prediction is achieved by SG-PLS for both nitrogen (*R*p=0.9049 and *RMSEP*=0.1041) and phosphorus (*R*p=0.9235 and *RMSEP*=0.0514) using the spectra data of the upper leaf side.

3.3 LS-SVM models

The RBF kernel function was used in LS-SVM models. The model parameters (γ, σ^2) were determined by a two-step grid search and cross-prediction process. The search region (γ, σ^2) was set from 10^{-4} to 10^4 for nitrogen and 10^{-3} to 10^3 for phosphorus. And the optimal γ and σ^2 thus obtained were 0.1 and 100, respectively. The prediction results for nitrogen and phosphorus in both the calibration and the prediction sets using the upper and lower leaf side spectral data are shown in Table 3. We can find from the results of LS-SVM models that the SG is also the best preprocessing method judging by prediction performance. In comparison, results of SG-PLS is better than SG-LS-SVM (*R*p=0.8962 and *RMSEP*=0.0179) in predicting nitrogen content using the upper side spectral data. In contrast, SG-LS-SVM got better prediction results for phosphorus (*R*p=0.9146 and *RMSEP*=0.2566) using the lower side spectral data, but its overall performance is worse than the SG-PLS.

Table 2 Prediction results of nitrogen and phosphorus by PLS using different preprocessing methods

Source of spectrum	Nutrient element	Preprocessing mothod	LVs	Calibration sample set		Prediction sample set	
				*R*c	*RMSECV*	*R*p	*RMSEP*
Upper side of leaf	Nitrogen	RAW	7	0.9452	0.1051	0.8935	0.1244
		SG	**8**	**0.9584**	**0.0915**	**0.9049**	**0.1041**
		MSC	11	0.5714	0.2539	0.7042	0.2024
		SNV	10	0.5023	0.2653	0.6575	0.2130
		1－Der	6	0.8000	0.1876	0.8272	0.1531
		2－Der	2	0.8354	0.1705	0.8129	0.167
	Phosphorus	RAW	8	0.9111	0.2377	0.9234	0.0515
		SG	**8**	**0.9109**	**0.238**	**0.9235**	**0.0514**
		MSC	11	0.8951	0.2571	0.7838	0.159
		SNV	13	0.9352	0.2043	0.8067	0.1465
		1－Der	6	0.9048	0.2456	0.8822	0.0782
		2－Der	2	0.8222	0.3283	0.839	0.1041
Lower side of leaf	Nitrogen	RAW	8	0.8536	0.1595	0.8038	0.1799
		SG	6	0.8368	0.1616	0.8149	0.0306
		MSC	9	0.806	0.1811	0.5757	0.0542
		SNV	9	0.8102	0.1794	0.5527	0.0582
		1－Der	3	0.7649	0.1971	0.7664	0.0419
		2－Der	3	0.7808	0.1912	0.753	0.0382
	Phosphorus	RAW	8	0.9221	0.2231	0.8341	0.124
		SG	7	0.9187	0.2278	0.8489	0.0118
		MSC	9	0.8703	0.2840	0.6061	0.2268
		SNV	9	0.8704	0.2840	0.6057	0.2278
		1－Der	3	0.8289	0.3226	0.7497	0.1908
		2－Der	6	0.9247	0.2196	0.7603	0.1679

Table 3 Prediction results of nitrogen and phosphorus by LS-SVM using different preprocessing methods

Leaf side	Nutrient element	Preprocessing method	LVs/(γ, σ^2)	Calibration sample set		Prediction sample set	
				*R*c	*RMSECV*	*R*p	*RMSEP*
Upper	Nitrogen	RAW	10/(6.2437, 22.3190)	0.8523	0.1601	0.8933	0.0154
		SG	10/(10.4135, 22.8921)	0.8615	0.1554	0.8962	0.0179
		MSC	3/(0.7229, 10.3051)	0.8593	0.1566	0.7705	0.0389
		SNV	3/(4.9196, 84.3228)	0.8406	0.1658	0.7436	0.0419
		1－Der	6/(1.9683, 24.9862)	0.8608	0.1558	0.8492	0.0210
		2－Der	6/(6.9329, 34.4926)	0.7680	0.1960	0.8283	0.0250
	Phosphorus	RAW	8/(5.9395, 23.8610)	0.9405	0.1995	0.8714	0.3067
		SG	8/(3.6748, 23.0513)	0.9347	0.2108	0.8706	0.3111
		MSC	5/(16.7512, 129.2642)	0.6731	0.4273	0.6856	0.4506
		SNV	5/(8.4065, 107.0960)	0.6690	0.4301	0.6835	0.4524
		1－Der	8/(5.1178, 29.6687)	0.8910	0.2646	0.8136	0.4077
		2－Der	8/(1.9976, 25.1116)	0.8157	0.3414	0.7368	0.4244
Lower	Nitrogen	RAW	5/(21.5122, 48.7186)	0.8714	0.1506	0.8317	0.1735
		SG	5/(10.4793, 32.0715)	0.8708	0.1512	0.8104	0.1738
		MSC	9/(3.8715, 30.5067)	0.3561	0.2688	0.7200	0.2157
		SNV	5/(9.9384, 47.4192)	0.6273	0.2389	0.5780	0.2247
		1－Der	8/(15.4215, 41.2877)	0.8603	0.1568	0.7839	0.2104
		2－Der	5/(13.2613, 38.9166)	0.7308	0.2100	0.7001	0.2058
	Phosphorus	RAW	9/(10.4135, 22.8921)	0.9374	0.1101	0.8957	0.1247
		SG	9/(2.2544, 20.4216)	0.9312	0.2236	0.9146	0.2566
		MSC	3/(0.5646, 3.6439)	0.6370	0.4522	0.6906	0.4417
		SNV	3/(0.5885, 4.0266)	0.6317	0.4540	0.6912	0.4414
		1－Der	5/(4.4448, 27.6468)	0.8270	0.3270	0.8395	0.3189
		2－Der	5/(15.3029, 58.9035)	0.8340	0.3195	0.8148	0.3424

3.4 Comparative analysis of the optimal models

Comparison of the prediction results nitrogen and phosphorus content by using spectrum information from both sides of leaves is shown in Table 4. The best prediction results were obtained by using SG-PLS (*R*p=0.9049 and *RMSEP*=0.1041) for nitrogen and PLS (*R*p=0.9235 and *RMSEP*=0.0514) for phosphorus respectively.

Table 4 Optimal modeling for prediction of nitrogen and phosphorus content in leaf

Leaf side	Nutrient element	Model	LVs/(γ, σ^2)	Calibration sample set		Prediction sample set	
				*R*c	*RMSECV*	*R*p	*RMSEP*
Upper	Nitrogen	SG-PLS	8	0.9584	0.0915	0.9049	0.1041
	Phosphorus	**PLS**	**8**	**0.9109**	**0.2380**	**0.9235**	**0.0514**
Lower	Nitrogen	LS-SVM	5/(21.5122, 48.7186)	0.8714	0.1506	0.8317	0.1735
	Phosphorus	SG -LS-SVM	9/(2.2544, 20.4216)	0.9312	0.2236	0.9146	0.2566

In this study, although the multivariate calibration models were used, better prediction results for nitrogen and phosphorus content are both based on the upper leaf reflective spectrum data. However, the reflectance data showed that the information extracted from the lower side of the citrus leaves (Figure 3-B_3) was more informative than that from the upper side (Figure 3-A_3). The possible explanations for the discrepancy would be:

1) The upper side is smoother with a thicker layer of wax, and the immediate underneath palisade tissue contains more chlorophyll and is more uniform in cell structure. These can contribute to stability of the reflectance spectral data, and thus enhanced the prediction accuracy. In contrast, the lower side is rougher, with cilia, oil glands and stomata and sponge tissues that contain less chlorophyll and is looser in cell structure. And all the structural uniformity of the lower leaf side can reduce the stability of the spectral data and the prediction power. Table 4 showed that the data of upper leaf side was suitable for multiple linear

regressions analysis (PLS) and the lower side data was better for nonlinear regression analysis (LS-SVM). Our results are consistent with the upper leaf side with a flatter surface and a higher pigment level which is suitable for extracting spectral data for multiple linear regression analysis[11,25].

2) As aforementioned, the pigment content in upper side is higher than in lower side[26]. This certain extent meant that the content of nitrogen and phosphorous is higher in the upper side potion and lower in the lower side potion.

These factors make the upper side spectral data of the leaf more powerful and robust than the lower side spectral data in building models for predicting leaf nutrient content[27]. The best scatter plots between predicted values and true content of nitrogen and phosphorus are shown in Figure 4 and Figure 5, respectively.

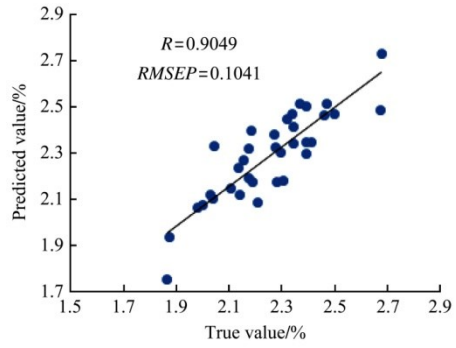

Figure 4 The best prediction result for nitrogen by SG-PLS model

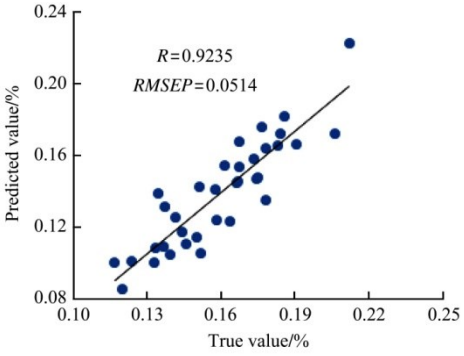

Figure 5 The best prediction result for phosphorus by PLS model

4 Conclusions

Hyperspectral imaging technique combined with chemometrics were used for nondestructive estimation of nitrogen and phosphorus content in leaf from both sides of the citrus leaves. The spectral data after preprocessed with different methods were compared for their accuracy in predicting nitrogen and phosphorus content in leaves by using PLS and LS-SVM models. The best prediction model is SG-PLS for nitrogen with *R*p=0.9049 and *RMSEP*=0.0138, and PLS for phosphorus with *R*p=0.9235 and *RMSEP*=0.0514. The results suggest:

1) The correlation is much stronger than several reported nitrogen and phosphorus content and its Vis/NIR spectra based on Hyperspectral imaging technique studies on in-field plants. Firstly, the hyperspectral data of the leaves was obtained by using the hyperspectral imaging system in lab which reduced the interference from the external environment in the study; secondly, we extracted a rectangular ROI which was manually selected with the method of double thresholds; thirdly, spectral pretreatment was performed to mathematically treat the extracted spectral data correct undesired effects such as light scattering and random noise resulting from variable physical sample properties or instrumental effects; fourthly, the set of individual leaves used in our study was small, that was why the correlation was much stronger than several reported nitrogen and phosphorus content and its Vis/NIR spectra based on Hyperspectral imaging technique studies on in-field plants;

2) The linear of PLS model and nonlinear of LS-SVM model fit better with spectral data of the upper side and lower side of leaves, respectively;

3) The hyperspectral imaging data from the upper side of leaves are better indicators of N and P content of leaves than those from lower side. In conclusion, using the hyperspectral data collecting and processing system to handle upper side of leaves can successfully get nutrition status of citrus leaves.

Acknowledgements

The authors thank the financial support from the International Science & Technology Cooperation program of China (2013DFA11470), International Science & Technology Cooperation Program of Chongqing (CSTC2011gjhz80001), National High Technology Research & Development Program of China (2012AA101904), Chongqing Science & Technology Project (cstc2012gg-yyis80002), Chongqing Science & Technology Support & Demonstration Project (CSTC2014fazktpt80015 & CSTC2014fazktjcsf80031).

[References]

[1] Vesna F, Heather O, George D, Hafizan J, Al C, Patricia C. Inorganic nitrogen, sterols and bacterial source tracking as tools to characterize water quality and possible contamination sources in surface water. Water Research, 2012; 46(4): 1079–1092.

[2] Goel P K, Prasher S O, Landry J A, Patel R M, Bonnell R B, Viau A A, et al. Potential of airborne hyperspectral remote sensing to detect nitrogen deficiency and weed infestation in corn. Computers and Electronics in Agriculture, 2003; 38(2): 99–124.

[3] Borin A, Ferro M F, Mello C, Maretto D A, Poppi R J. Least-squares support vector machines and near infrared spectroscopy for quantification of common adulterants in powdered milk. Analytica Chimica Acta, 2006; 579(1): 25–32.

[4] Dae Gwan Kim, Thomas F. Burks, Jianwei Qin, Duke M. Bulanon Classification of grapefruit peel diseases using color texture feature analysis Int J Agric & Biol Eng, 2009; 2(3): 41–50.

[5] Min M, Lee W S, Burks T F, Jordan J D, Schumann A W, Schueller J K, et al. Design of a hyperspectral nitrogen sensing system for orange leaves. Computers and Electronics in Agriculture, 2008; 63(2): 215–226.

[6] Congalton R G, Mead R A. A quantitative method to test for consistency and correctness in photointerpretation. Photogrammetric Eng. Remote Sens., 1983; 49(1): 69–74.

[7] Vyacheslav N K, Nick S. On the origin of the spectral bands in the visible absorption spectra of visible-light-active TiO_2 specimens analysis and assignments. The Journal of Physical Chemistry C, 2009; 113(34): 15110–15123.

[8] Lü Q, Cai J R, Liu B, Deng L, Zhang Y J. Identification of fruit and branch in natural scenes for citrus harvesting robot using machine vision and support vector machine Int J Agric & Biol Eng, 2014; 7(2): 115-121.

[9] Xiao B, Mao W H, Liang X H, Zhang L J, Han L B. Study on Varieties Identification of Kentucky Bluegrass Using Hyperspectral Imaging Discriminant Analysis. Spectroscopy and spectral Analysis, 2012; 32(6): 1620–1623. (in Chinese with English abstract)

[10] Wang D, Ding Y S, Guo Z H, Min S G The application of near-infrared spectra micro-image in the imaging analysis of biology samples Journal of Innovative Optical Health Sciences, 2014; 7(4): 10-20.

[11] Chai A L, Li B J, Wang Q, Shi Y X, Huang H Y. Detecting chlorophyll content of tomato leaves with technology of computer vision. Acta Horticulturae Sinica, 2009; 36(1): 45–52. (in Chinese with English abstract)

[12] Wang K R, Li S K, Wang C T, Yang L, Xie R Z, Gao S J, et al. Acquired chlorophyll concentration of cotton leaves with technology of machine vision. Acta Agronomica Sinica, 2005; 32(1): 34–40. (in Chinese with English abstract)

[13] Tong Z. Research on the Leaves Information of Rice Based on Computer Vision. Postgraduate dissertation. Hunan: Hunan Agricultural University, 2010. (in Chinese with English abstract)

[14] Clevers J, Kooistra L. Using hyperspectral remote sensing data for retrieving canopy chlorophyll and nitrogen content. Selected Topics in Applied Earth Observations and Remote Sensing, Journal of IEEE, 2012; 5(2): 574–583.

[15] Liu F, Nie P C, Huang M, Kong W W, He Y. Nondestructive determination of nutritional information in oilseed rape leaves using visible/near infrared spectroscopy and multivariate calibrations. Science China Information Sciences, 2011; 54(3): 598–608.

[16] Dawson T P, Curran P J, Plummer S E. LIBERTY-Modeling the effects of leaf biochemical concentration on reflectance spectra. Remote Sensing of Environment, 1998; 65(1): 50–60.

[17] Guo Z M, Huang W Q, Chen L P, Peng Y K, Wang X. Shortwave infrared hyperspectral imaging for detection of pH value in Fuji apple. Int J Agric & Biol Eng, 2014; 7(2): 130–137.

[18] Dhanoa M S, Lister S J, Sanderson R, Barnes R. The link between multiplicative scatter correction (MSC) and standard normal variate (SNV) transformations of NIR spectra. Journal of Near Infrared Spectroscopy, 1994; 2(1): 43–47.

[19] Chu X L, Yuan H F, Lu W Z. Progress and application of spectral data pretreatment and wavelength selection methods in NIR analytical technique. Progress in Chemistry, 2004; 16(4): 528–542. (in Chinese with English abstract)

[20] Ni Y N, Mei M H, Kokot S. Analysis of complex, processed substances with the use of NIR spectroscopy and chemometrics: Classification and prediction of properties-The potato crisps example. Chemometrics and Intelligent Laboratory Systems, 2011; 105(2): 147–156. (in Chinese with English abstract)

[21] Balabin R M, Lomakina E I. Support vector machine regression (LS-SVM)-an alternative to artificial neural networks (ANNs) for the analysis of quantum chemistry data. Physical Chemistry Chemical Physics, 2011; 13(24): 11710–11718.

[22] Suykens J A K, Van Gestel T, De Brabanter J, De Moor B, Vandewalle J. Least squares support vector machines. Singapore: World Scientific, 2002.

[23] Wu D, He Y, Feng S. Short-wave near-infrared spectroscopy analysis of major compounds in milk powder and wavelength assignment. Analytica Chimica Acta, 2008; 610(2): 232–242. (in Chinese with English abstract)

[24] Balabin R M, Lomakina E I. Support vector machine regression (SVR/LS-SVM)-an alternative to neural networks (ANN) for analytical chemistry Comparison of nonlinear methods on near infrared (NIR) spectroscopy data. The Analyst, 2011; 136(8): 1703–1712.

[25] Niklas K J. Plant biomechanics: an engineering approach to plant form and function. Chicago: University of Chicago press, 1992.

[26] Harb J, Kittemann D, Neuwald DA, Hoffmann T, Schwab W. Correlation between Changes in Polyphenol Composition of Peels and Incidence of CO_2 Skin Burning of 'Cameo' Apples As Influenced by Controlled Atmosphere Storage. Journal of agricultural and food chemistry, 2013; 61(15): 3624–3630.

[27] Lang Y Z, Zhang Z J, Gu X Y, Yang J C, Zhu Q S. Physiological and Ecological Effects of Crimpy Leaf Character in Rice (Oryza sativa L.) Ⅱ. Photosynthetic Character, Dry Mass Production and Yield Forming. Acta Agronomica Sinica, 2004; 30(8): 739–744. (in Chinese with English abstract)